Hindawi
Adsorption Science & Technology
Volume 2022, Article ID 9366899, 9 pages
https://doi.org/10.1155/2022/9366899

Research Article

Synthesis and Optimization of Cr (VI) Removal from Aqueous Solution by Activated Carbon with Magnetic Fe_3O_4Nanoparticles by Response Surface Methodology

L. Natrayan,[1] **R. Rajalakshmi**,[2] **K. Amandeep Singh**,[2] **Pravin P. Patil**,[3] **Dhinakaran Veeman**,[4] **and Prabhu Paramasivam**[5]

[1]*Department of Mechanical Engineering, Saveetha School of Engineering, SIMATS, Chennai, 602105 Tamil Nadu, India*
[2]*Department of Computer Science and Engineering, Sathyabama Institute of Science and Technology, Chennai, Tamil Nadu, India*
[3]*Department of Mechanical Engineering, Graphic Era Deemed to Be University, Bell Road, Clement Town, 248002 Dehradun, Uttarakhand, India*
[4]*Centre for Additive Manufacturing, Chennai Institute of Technology, 600069, Chennai, Tamil Nadu, India*
[5]*Department of Mechanical Engineering, College of Engineering and Technology, Mettu University, Ethiopia 318*

Correspondence should be addressed to Prabhu Paramasivam; prabhu.paramasivam@meu.edu.et

Received 31 December 2021; Revised 18 February 2022; Accepted 4 March 2022; Published 17 March 2022

Academic Editor: Lakshmipathy R

In this study, the activated carbon with Fe_3O_4 nanoparticles was synthesized and employed as an effective tool to remove the Cr (VI) from the aqueous solution. The process inputs like concentration of Cr (VI), the dosage of Fe_3O_4 nanoparticles in activated carbon, and pH of the aqueous solution were optimized by response surface methodology, and their effects were studied. The statistical analysis by ANOVA showed that the process inputs were significantly affected the removal rate, with the maximum impact provided by the pH of the aqueous solution. The best parameters were identified to be pH of 3, aqueous solution concentration of 12 mg/L, the dosage of 1.5 g/L, and adsorption time of 40 min. SEM, EDS, and FTIR characterized the synthesized activated carbon/Fe_3O_4 samples with magnetic characteristics. Adsorption isotherms and adsorption kinetics analyzed the chemical stability of the synthesized nanocomposite.

1. Introduction

The contamination of water due to the dumping of industrial wastes with heavy metals like arsenic, chromium, mercury, and lead into water bodies has been a major concern because of their toxic and carcinogenic effects on human health [1]. Chromium, one of the most dangerous heavy metals, is released into the water bodies in the form of Cr (VI) by the steel, dyeing industry, tanning, electroplating, and chromate synthesis industries [2]. Cr (VI) is more toxic than Cr (III), and its presence in water and soil in the range of 5-220 mg/L has been reported to cause pollution [3]; the Cr (VI) has higher water solubility, which affects the kidney and liver and causes dermatologic ailments [4]. Therefore, considering such issues, the requirement to resolve the problem by identifying effective techniques to remove the heavy metals from water bodies was stressed [5].

Various processes to remove the heavy metals like ion exchange, chelation, chemical precipitation [6], electrochemical treatment [7], reverse osmosis [8], membrane separation [9], and biosorption were employed [10]. However, these techniques possessed constraints like increased capital costs, equipment costs, high maintenance costs, poor material removal, etc. [11]. Adsorption is the most commonly employed technique to remove heavy metals from the aqueous solutions due to their ease of operation [12], low costs, and high efficiency [13]. Activated carbon is commonly employed to remove the heavy metals in water bodies due to its high porosity, high surface area, increased absorptivity, and high stability to thermal and chemical attacks

Table 1: Experimentation runs with results.

Run no.	Concentration, mg/L	Adsorption time, min	Dosage, g/L	pH	*R* %
1	7.5	40	1.5	6	44.35
2	3	40	1.5	9	65.49
3	3	40	2.25	6	67.56
4	7.5	20	1.5	3	65.98
5	7.5	40	2.25	3	84.78
6	7.5	40	1.5	6	45.3
7	3	40	1.5	3	65.6
8	7.5	20	0.75	6	74.7
9	3	40	0.75	6	42.8
10	7.5	60	1.5	3	75.38
11	7.5	40	2.25	9	10.2
12	7.5	60	1.5	9	60.4
13	7.5	60	0.75	6	47.32
14	7.5	40	1.5	6	42.5
15	7.5	40	1.5	6	66.37
16	12	60	1.5	6	64.32
17	3	20	1.5	6	45.89
18	12	40	1.5	3	99.21
19	7.5	20	2.25	6	25.32
20	12	40	2.25	6	45.5
21	7.5	40	0.75	9	67.2
22	12	20	1.5	6	84.5
23	7.5	20	1.5	9	42.8
24	7.5	40	1.5	6	44.2
25	3	60	1.5	6	88.78
26	12	40	1.5	9	54.2
27	12	40	0.75	6	73.2
28	7.5	60	2.25	6	75.2
29	7.5	40	0.75	3	43.2

[14]. Such characteristics of activated carbon make it a viable option in pharmaceutical, chemical, food, petroleum, and treatment of industrial, urban, and suburban waters. Activated carbon can remove solid and gaseous wastes and recover vital elements [15]. Wang et al. employed activated carbon produced from bamboo and coated with Co. The composite was heated with the assistance of microwaves. The adsorbent showed good adsorption results with the Co^{2+} ion facility ion exchange. Despite such beneficial properties of activated carbon, the activated carbon needs to be enhanced [16]. Several enhancement techniques, such as acid/base treatments, ozone, plasma and microwave processing, metal, metal oxide, and nanoparticle impregnation, are employed [17]. Adebayo et al. reported the effects of heavy Cr (VI) ions by synthesizing the activated carbon from tree bark, goethite, and their composite. The authors observed good adsorption of Cr (VI) ions by both goethites and activated carbon [18]. Nasseh et al. produced activated carbon-based agricultural wastes. The authors observed good adsorption by the powdered activated carbon [19].

Moreover, the authors recommended ultrasonic activation to remove the waste water's Cr (VI) ions. Bharath et al. studied the influence of process variables in removing Cr (VI) ions by the magnetic nanocomposite synthesized by impregnating Fe_3O_4 in activated carbon synthesized from peanut shells [20]. Wang et al. used activated carbon for the removal of heavy metal ions. The authors observed that the diffusion occurred initially through the pores and then by the surface [21]. Kumar and Jena achieved a higher adsorption rate by chemically activating the activated carbon with the help of $ZnCl_2$. The authors observed that the pH, concentration, and temperature significantly affected the adsorption rate [22]. Doke and Khan studied the chemical kinetics in the adsorption of heavy Cr (VI) ions by activated carbon produced from applewood shells. The authors could achieve higher adsorption at the low quantitate of activated carbon [23]. Manjuladevi et al. reported the effects of process variables on the adsorption of heavy metals like Cr, Ni, Pb, etc. with the help of activated carbon synthesized from Cucumis melo peel.

Jain et al. characterized the adsorption of heavy metals by Fe3O4 impregnated activated carbon. The authors identified that the concentration, dosage, pH, and contact time were key process variables [24]. The authors produced good repeatability in the regeneration of the nanocomposite [25]. The techniques above, metal and metal oxide-based nanoparticle impregnation is getting increased attention because of their increased adsorption capacity [26]. However, the recovery of these devices is difficult from the water bodies. This issue was overcome with the magnetic nanoparticle enhanced activated carbon, as these devices could be easily recoverable and offered higher surface area [27].. The Fe_3O_4 was observed to yield better results when impregnated with activated carbon [28].

The current research article presents the research on the absorptivity of Cr (VI) ions from water using the fabricated nanocomposite of Fe3O4 + activated carbon. The activated carbon with Fe3O4 nanoparticle's performance was highly dependent on the process inputs, which stressed the need for process optimization to determine the most feasible conditions [29]. Various optimization techniques like Taguchi and response surface methodology were employed by the researchers to identify the best process variables. Also, these techniques helped the users to understand the interactive effects of the process variables on the response [30] inputs like concentrate.

2. Materials and Methods

2.1. Production of Activated Carbon. The sludge obtained from the paper mill was used to synthesize the activated carbon. The synthesis was based on the mechanism followed by Gorzin and Adadi [4]. The raw materials were dried at a temperature of 110°C for 24 hr. in an oven. The drying stage was followed by crushing and sieving to obtain the desired size of the particles. The obtained product was chemically activated, soaked in a 5 M zinc chloride solution in a mass ratio of 1 : 3, and mixed for eight hr. at a temperature of 85°C with the assistance of a magnetic stirrer. After the

Table 2: ANOVA results.

Source	Sum of squares	Df	Mean square	F value	p value	
Model	10291.06	14	735.08	18.27	<0.0001	Significant
A, concentration	167.33	1	167.33	4.16	0.0608	
B, adsorption time	434.52	1	434.52	10.8	0.0054	
C, dosage	132.4	1	132.4	3.29	0.0912	
D, pH	1493.21	1	1493.21	37.11	<0.0001	
AB	994.46	1	994.46	24.72	0.0002	
AC	688.01	1	688.01	17.1	0.001	
AD	504	1	504	12.53	0.0033	
BC	1492.28	1	1492.28	37.09	<0.0001	
BD	16.81	1	16.81	0.4178	0.5285	
CD	2429.5	1	2429.5	60.38	<0.0001	
A^2	1294.86	1	1294.86	32.18	<0.0001	
B^2	449.15	1	449.15	11.16	0.0048	
C^2	74.1	1	74.1	1.84	0.1962	
D^2	257.66	1	257.66	6.4	0.024	
Residual	563.29	14	40.24			
Lack of fit	162.01	10	16.2	0.1615	0.991	Not significant
Pure error	401.28	4	100.32			
Cor total	10854.35	28				

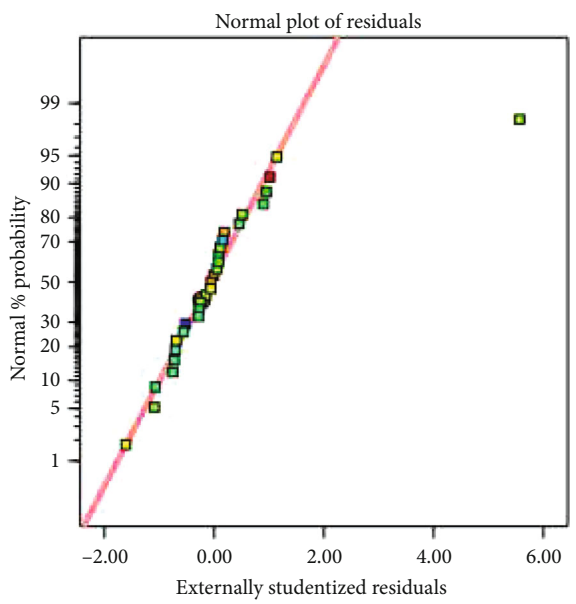

Figure 1: Experimental vs. predicted adsorption.

chemical activation, the product was oven-dried at a temperature of 120°C for 24 hours. The carbonization process for the product was done in an inert atmosphere with a nitrogen gas flow of 0.5 L/min in a furnace for 650°C for an hour at a heating rate of 20°C/min. Postcarbonization, the product was cooled on the surface to room temperature with the nitrogen gas flow [31]. The cooled product was washed by 1 M HCl and filtered and rinsed in warm water to obtain the neutral pH and filter the inorganic residue. The obtained product was then oven-dried at 120°C.

2.2. Chemicals. The compounds ammonium hydroxide (NH_4OH), copper nitrate (Cu $(No_3)_2$), ferric sulphate ($FeSO_4$), ferric chloride ($FeCl_3$), hydrochloric acid (HCl), 0.1 M sodium hydroxide (NaOH), and activated carbon were used in this study.

2.3. Synthesis and Characterization of Magnetic Fe_3O_4 Nanoparticle with Activated Carbon. The synthesis of magnetic nanoparticles with homogeneous composition and narrow size distribution was done by active coprecipitation under alkaline conditions [14]. Under an inert environment, the compounds $FeSO_4.7\ H_2O$ of 2.5 g, $FeCl_3.6H_2O$ of 3.5 g, and activated carbon of 12 g were dissolved in double distilled water and were subjected to strong stirring [32]. The solution was heated to 80°C; 10 mL NH_4OH was further combined with the chemical reactivity for 0.5 hr. The solution was cooled to collect the residue and persistently treated with ddH_2O. The synthesized activated carbon impregnated with magnetic Fe_3O_4 nanoparticles was characterized using SEM and FTIR.

2.4. Adsorption Experimentation. Adsorption experiments were done by varying the amounts of activated carbon impregnated with magnetic Fe_3O_4 nanoparticles and aqueous solution with Cr (VI) at 27 ± 1°C agitated at 150 RPM and varying pH range. The obtained solution is subjected to centrifugal force by a centrifuge to obtain the nanocomposite [33]. The product was then subjected to flame atomic separation. The removal of Cr (VI) ions was computed as follows:

$$R\% = \frac{C_0 - C_e}{C_0} \times 100. \quad (1)$$

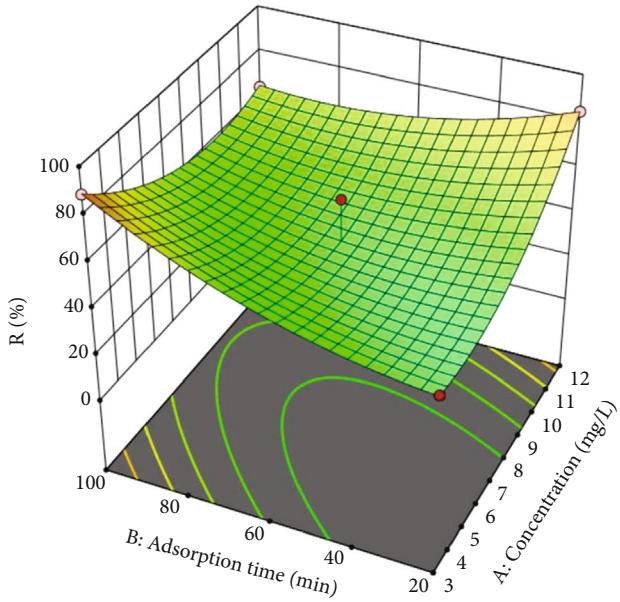

Figure 2: Effects of adsorption time and concentration on adsorption rate.

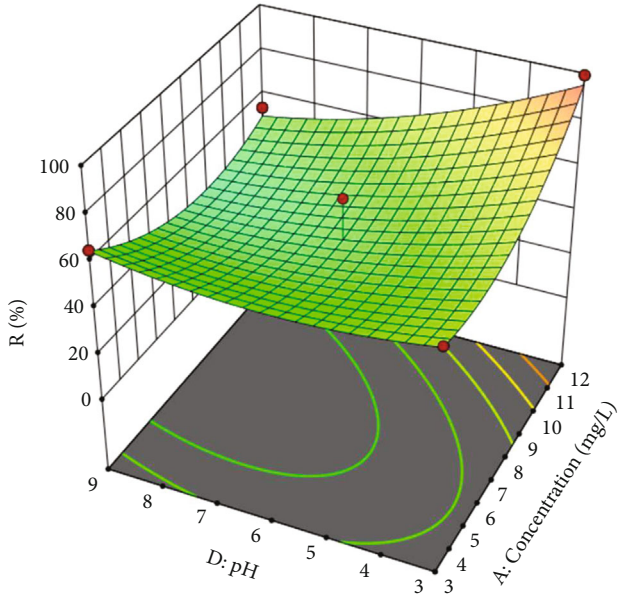

Figure 3: Effects of pH and concentration on adsorption rate.

C_0 and C_e are initial concentration and equilibrium concentration of Cr (VI), mg/L, respectively; V is the volume of the solution, L.

2.5. Response Surface Methodology (RSM). Response surface methodology is an optimization technique that helps the user determine the most significant processing conditions in an experiment where several process variables influence the outcome [34]. The experiments were carried out based on the Box-Behnken experimental design. The preliminary experiments showed that process variables like concentration of Cr (VI), the dosage of Fe_3O_4 nanoparticles, absorption time, and pH of the aqueous solution showed a critical impact on the adsorption rate. Therefore, these parameters were considered for the optimization study. Totally 29 experiments were carried out based on the Box-Behnken experimental design. The analysis of variance (ANOVA) at 95% confidence level was employed to study the statistical stability of the experimental design experimental runs. The results are presented in Table 1, and the ANOVA is presented in Table 2. The experimental design was generated using the Design Expert 11 statistical software [35].

The maximum absorptivity of 99.21% was observed at 12 mg/L concentration, 40 min adsorption time, and 1.5 g/L dosages, and pH of a solution of a developed mathematical model based on the quadratic regression equation is presented as follows:

$$\begin{aligned} R\% = {} & -3.35019 + 8.1897\,A - 2.18593\,B + 56.95511\,C \\ & + 9.17767\,D - 0.175194\,AB - 3.8893\,AC - 0.831481\,AD \\ & + 1.28767\,BC + 0.0341167\,BD - 10.95333\,CD \\ & + 0.697720\,A^2 + 0.020803\,B^2 - 6.00874\,C^2 + 0.700827\,D^2. \end{aligned} \quad (2)$$

From Table 2, it is observed that the adsorption time and pH of the solution were the most significant process variable which had a statistical influence on the experimentation. Moreover, the R_{sq} and R_{aj-sq} were observed to be 0.95 and 0.9. The high values of the regression coefficients showed that the experimentation is statistically satisfactory. The interactions of the process variables AB, AD, BC, and CD were identified as the important terms, considering their p values < 0.05. The predictability of the RSM was also observed to be closer to the experimental adsorption values, as seen in Figure 1.

3. Results and Discussions

3.1. Effects of Process Variables on Adsorption. The benefits of employing the response surface methodology to the user are the generation of the 3D plots, which help understand the effects of interactions of the process variables on the process outcome.

Figure 2 shows the effects of concentration and adsorption time on the adsorption percentage. It is observed that the increase in the concentration of the aqueous solution and the adsorption time, the adsorption rate increases a trend can be credited to the sufficient time available for the chemical interaction between the synthesized nanocomposite and the aqueous solution to absorb higher amounts of Cr (VI).

Figure 3 shows the effects of pH and the concentration on the adsorption rate. The adsorption rate was low with the increase in the pH and low concentration. This trend can be credited to the higher presence of the acid content had the upper hand in the chemical reactions to dent the adsorption. However, the increase in the concentration at lower pH was observed to improve the adsorption rate. The lower acid levels enabled increased chemical reactivity

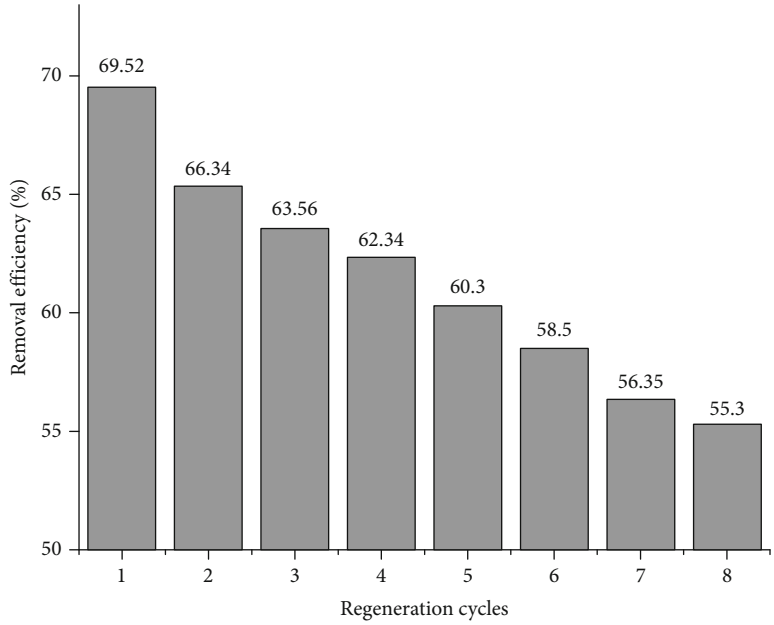

Figure 4: Effect of regeneration cycles on the removal of Cr (VI) by activated carbon with Fe3O4 nanocomposite.

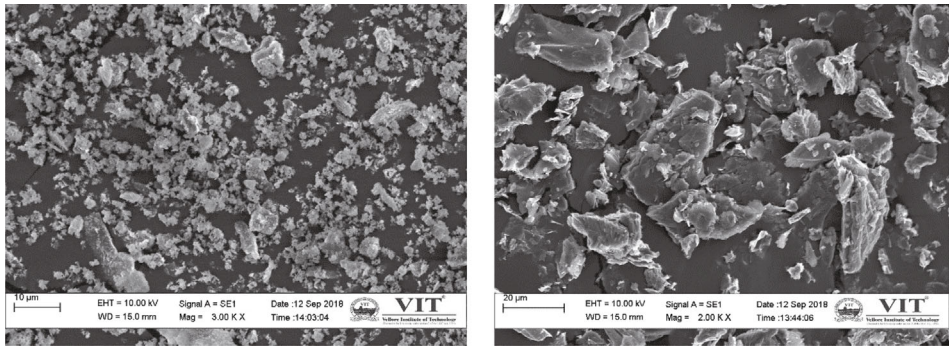

Figure 5: SEM micrograph of the activated carbon.

between the activated carbon and Fe_3O_4 magnetic nanoparticle to increase the adsorption of Cr (VI).

3.2. Confirmation Test Experimentation. The confirmation test experimentation was carried out at the concentration level of 12 mg/L, adsorption time of 40 min, 1.5 g/L dosages of Fe_3O_4, and pH of 3, with an adsorption percentage of 99.21%. The predicted value by RSM at these conditions was 95.05%. The confirmation tests at these conditions showed an adsorption percentage of 97.56%. The confirmation test values show that the RSM is an effective system to optimize and predict the adsorption rate. The comparison study was done to compare the performance of the synthesized composite with the results from the literature. The result obtained in the current study was in agreement with the result obtained by Guo et al., where the authors used cassava sludge-based adsorbent.

3.3. Reusability Studies. The reusability study is vital considering the factory applications. Analyze the reusability of the activated carbon with Fe_3O_4 nanoparticle as an adsorbing agent, the regeneration study was carried out, and results are exposed in Figure 4. The adsorption rate of Cr (VI) by the activated carbon with Fe_3O_4 was observed to fall with the increase in the regenerating times. However, the adsorption rate was measured to be 73.5%. The adsorption rate was measured for 5 repeated cycles. The regeneration analysis shows that the activated carbon impregnated with Fe_3O_4 nanoparticle is an effective chemical composite to remove the Cr (VI) from water bodies.

3.4. Morphological Analysis. Figure 5 shows that the SEM micrograph of the activated carbon was observed with the pore formation on the surface. The diameter of Fe_3O_4 nanoparticles dispersed on the surface of activated was in the range of 30-60 nm. The average diameter of the activated carbon with the Fe_3O_4 was found to be 42 nm. The EDS analysis confirmed the adsorption of the Cr (VI) ions by the Fe_3O_4 impregnated in activated carbon nanocomposite. The adsorption was determined by comparing the EDS of the experimented sample and the untested sample. The coprecipitation technique in the aqueous solution was the

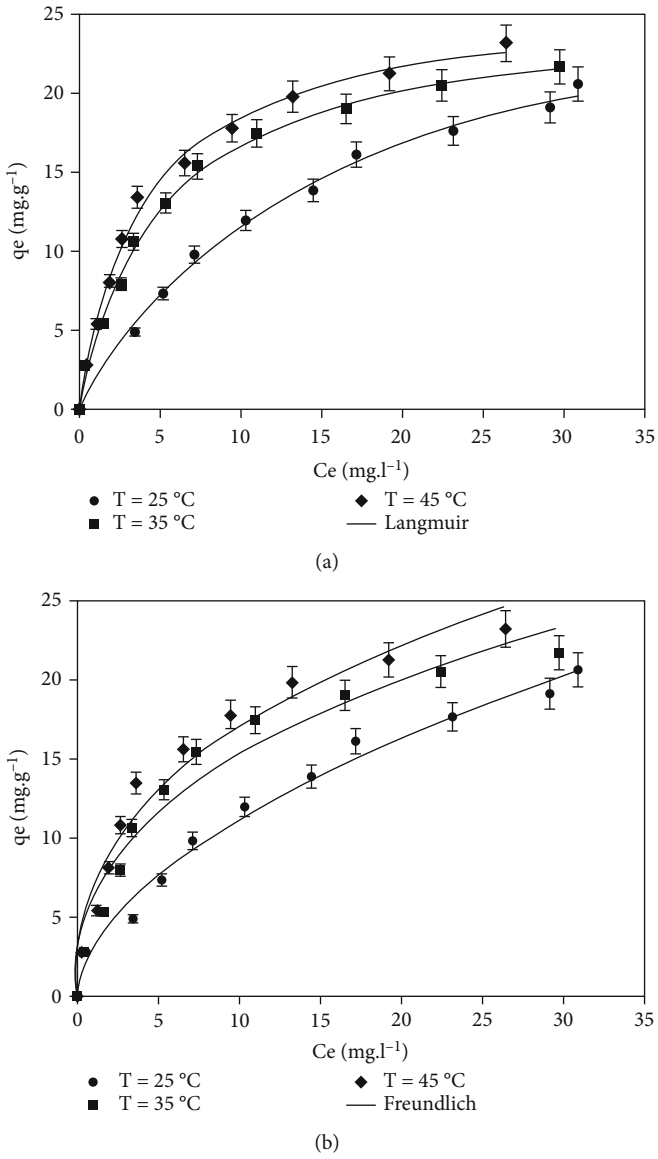

Figure 6: (a) Langmuir and (b) Freundlich isotherm curves at the values for best adsorption.

used and effective technique to obtain the magnetic nanoparticles. The produced magnetic nanoparticles by coprecipitation technique dispersed on the activated carbon had a fair distribution. Moreover, the uniform dispersion of the Fe_3O_4 nanoparticles in the activated carbon showed controlled aggregation produced by the activated carbon [14].

The SEM results confirmed the formation of the Fe_3O_4 impregnated in activated carbon magnetic nanocomposite. The wavenumbers in the FTIR spectra were found to be 500 to 5000 cm^{-1}. The adsorption band was approximately found to be at 3445 cm^{-1}, which is wider and broader. Such a trend in adsorption was due to the adsorption of the water on the activated carbon surface and extending vibration of oxygen-hydrogen bond in the water molecule. For the magnetic Fe_3O_4 nanoparticle, the adsorption peaks were found at approximately 684, 450, and 814 cm^{-1} because of the extension of the iron-oxygen bond in Fe_3O_4. The peaks approximately at 1378 cm^{-1} were hydrocarbon groups (CH_2 and CH_3), whereas at ~1657 cm^{-1} and 983 cm^{-1} were contributed by the extension of the carbon-oxygen bond aliphatic carbon-nitrogen bond, respectively.

3.5. Adsorption Isotherms. The absorptivity of Cr (VI) by Fe_3O_4 impregnated in activated carbon magnetic nanocomposite and its concentration was studied with the help of adsorption isotherms [4]. The obtained experimental results for Cr (VI) adsorption were analyzed using Langmuir and Freundlich expression [36], which is expressed in equation (3) and Figures 6(a) and 6(b).

$$q_e = \frac{q_{\max} b C_e}{1 + b C_e}, \tag{3}$$

where q_e is the quantity of Cr (VI) ions adsorbed/unit weight at equilibrium (mg/g). $q_{\max}$ is the peak adsorption (mg/g), C_e is the equilibrium of Cr (VI) ion concentration (mg/L), and

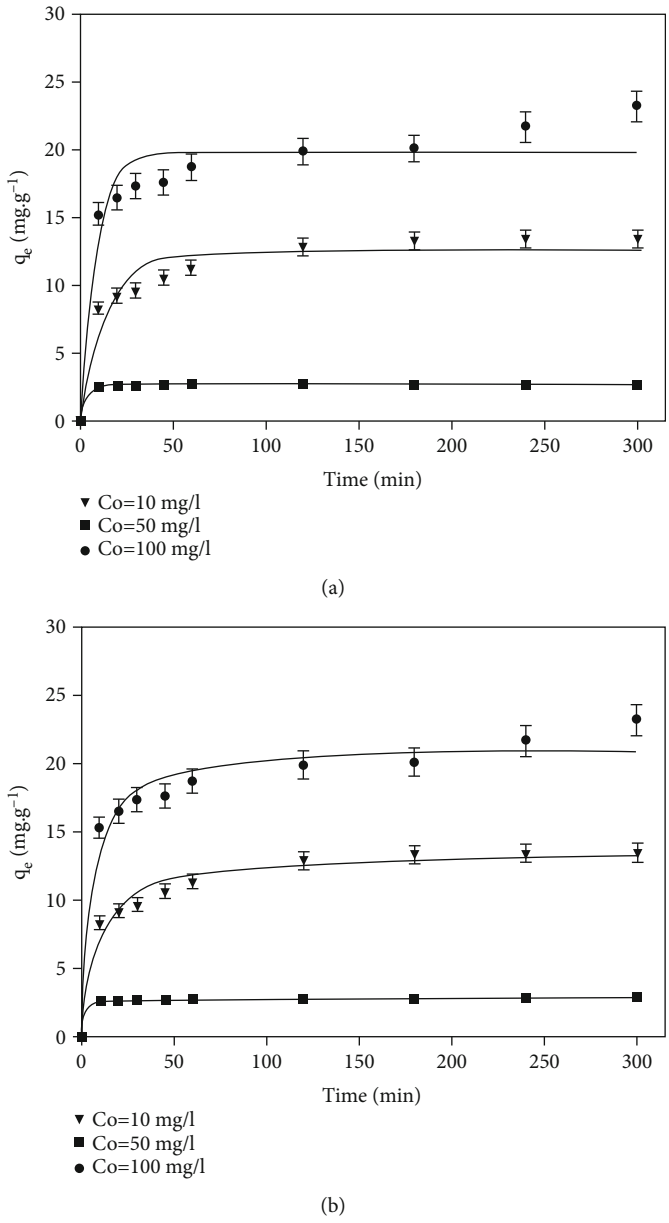

Figure 7: (a) Pseudo 1st order kinetic model and (b) pseudo 2nd order kinetic model for the best adsorption condition.

b is Langmuir constant associated with the bonding energy of Cr (VI) ion (L/mg).

The adsorption on the multilayer surface is presented by the Freundlich expression (equation (4)).

$$q_e = K_f C_e^{1/n}, \tag{4}$$

where K_f(mg/g (1 m/g)$^{1/n}$) and n are Freundlich constant, indicators of the adsorption rate, and intensity, respectively.

The curve parameters and the nonlinearity, R^2 (Langmuir constants), observed as $b = 0.0572$ (L/mg), $q_{max} = 31.59$ (mg/g), relative error = 0.039, and $R^2 = 0.9841$, whereas, Freundlich constants, $K_f = 3.5865$ (mg/g (1 m/g)$^{1/n}$), $n = 1.89$, relative error = 0.063, and $R^2 = 0.9822$.

The influence of milling tool coatings and holder coatings in CNC milling on surface roughness has been discussed by Bejaxhin and Paulraj, with some optimum outcomes that may also be confirmed with experimental results. The dynamic simulation can also be confirmed with the experimental component, which depicts variations in surface roughness due to coating effects in the tool and holder assembly [37].

3.6. Adsorption Kinetics. Adsorption of the Cr (VI) ions by Fe_3O_4 impregnated in activated carbon magnetic nanocomposite; adsorption kinetics provide a better understanding of this phenomenon [4, 28–33]. Adsorption of Cr (VI) ions, the pseudo 1st order, and pseudo 2nd order models was employed to test the experimental information. The

nonlinear terms of pseudo 1st order and pseudo 2nd order are determined as follows:

$$q_t = q_e\left(1 - e^{-k_1 t}\right), \tag{5}$$

$$q_t = \frac{k_2 q_e^2}{1 + k_2 q_e t} t, \tag{6}$$

where q_t and q_e (mg/g) represent the adsorption capacities at equilibrium and time, t, min, respectively, k_1 (1/min) represent the pseudo 1st order constant, and k_2 (g/mg/min) represent the pseudo 2nd order constant. The nonlinear patterns are presented in Figures 7(a) and 7(b). The origin plotting tool was employed to fit the curve to determine the constants. The R^2 and the adsorption capacities of the pseudo 1st order were q_e expected of 3.1 mg/g and $q_e$computed of 2.98 mg/g, with R^2 of 0.991, whereas for the pseudo 2nd order were q_e computed of 2.92 mg/g, k_2 of 0.0421, and with R^2 of 0.9984. From the values, it is observed that the pseudo 1st order model was inappropriate for modelling Cr (VI) adsorption. From the values of 2nd order, a better correlation of the experimental information is seen, which suggests that the Cr (VI) adsorption is based on chemisorption. Bejaxhin and Paulraj employed microphone audio signals with coated utensils to experimentally verify the vibration levels of CNC milling machines, and the signal frequency may be used to compare the surface quality of machined slots. The optimization can also be utilised to quickly identify factors that influence machine character and surface quality [38].

4. Conclusions

The activated carbon was impregnated with Fe_3O_4 magnetic nanoparticles to remove the Cr (VI) ions from the water bodies via a cost-effective technique. The response surface methodology determined the best adsorption conditions of pH of 3, aqueous solution concentration of 12 mg/L, the dosage of 1.5 g/L, and adsorption time of 40 min. FTIR results confirmed the formation of the activated carbon impregnated with Fe_3O_4 magnetic nanocomposite. The average diameter of the dispersed nanoparticle was measured to be 42 nm. The regeneration experiments showed good repeatability, which showed that the synthesized nanocomposite effectively removed the Cr (VI) ions. The chemical kinetics study showed that the fabricated nanocomposite was chemically stable to adsorb the heavy metal ions onto the surface.

Data Availability

The data used to support the findings of this study are included within the article. Should further data or information be required, these are available from the corresponding author upon request.

Disclosure

It was performed as a part of the employment of Mettu University, Ethiopia.

Conflicts of Interest

The authors declare that there are no conflicts of interest regarding the publication of this paper.

Acknowledgments

The authors thank Saveetha School of Engineering, SIMATS, Chennai, for the technical assistance. The authors appreciate the support from Mettu University, Ethiopia.

References

[1] H. Sharififard, M. Nabavinia, and M. Soleimani, "Evaluation of adsorption efficiency of activated carbon/chitosan composite for removal of Cr (VI) and Cd (II) from single and bi-solute dilute solution," *Advances in environmental technology*, vol. 2, no. 4, pp. 215–227, 2017.

[2] Y. Devarajan, B. Nagappan, G. Choubey, S. Vellaiyan, and K. Mehar, "Renewable pathway and twin fueling approach on ignition analysis of a dual-fuelled compression ignition engine," *Energy & Fuels*, vol. 35, no. 12, pp. 9930–9936, 2021.

[3] T. A. Saleh and V. K. Gupta, "Column with CNT/magnesium oxide composite for lead (II) removal from water," *Environmental Science and Pollution Research*, vol. 19, no. 4, pp. 1224–1228, 2012.

[4] F. Gorzin and M. M. Bahri Rasht Abadi, "Adsorption of Cr (VI) from aqueous solution by adsorbent prepared from paper mill sludge: kinetics and thermodynamics studies," *Adsorption Science & Technology*, vol. 36, no. 1-2, pp. 149–169, 2018.

[5] Y. Devarajan, D. B. Munuswamy, B. T. Nalla, G. Choubey, R. Mishra, and S. Vellaiyan, "Experimental analysis of Sterculia foetida biodiesel and butanol blends as a renewable and eco-friendly fuel," *Industrial Crops and Products*, vol. 178, p. 114612, 2022.

[6] J. Yang, M. Yu, and W. Chen, "Adsorption of hexavalent chromium from aqueous solution by activated carbon prepared from longan seed: kinetics, equilibrium and thermodynamics," *Journal of Industrial and Engineering Chemistry*, vol. 21, pp. 414–422, 2015.

[7] V. Gayatri, N. Bhanu Teja, D. K. Sharma, J. Thangaraja, and Y. Devarjan, "Production of biodiesel from Phoenix sylvestris oil: process optimisation technique," *Sustainable Chemistry and Pharmacy*, vol. 26, p. 100636, 2022.

[8] S. Mozaffari, M. Chaloosi, F. Divsar et al., "Spectrophotometric study of complexation of tri-aza dibenzosulfide and dibenzosulfoxide macrocyclic compounds with heavy metal ions," *Phosphorus, Sulfur, and Silicon and the Related Elements*, vol. 182, no. 10, pp. 2439–2448, 2008.

[9] Y. Devarajan, G. Choubey, and K. Mehar, "Ignition analysis on neat alcohols and biodiesel blends propelled research compression ignition engine," *Energy Sources, Part A: Recovery, Utilization, and Environmental Effects*, vol. 42, no. 23, pp. 2911–2922, 2020.

[10] M. Hunsom, K. Pruksathorn, S. Damronglerd, H. Vergnes, and P. Duverneuil, "Electrochemical treatment of heavy metals (Cu2+, Cr6+, Ni2+) from industrial effluent and modeling of

copper reduction," *Water Research*, vol. 39, no. 4, pp. 610–616, 2005.

[11] S. Justin Abraham Baby, S. Suresh Babu, and Y. Devarajan, "Performance study of neat biodiesel-gas fuelled diesel engine," *International Journal of Ambient Energy*, vol. 42, no. 3, pp. 269–273, 2021.

[12] D. Bolzonella, F. Fatone, S. di Fabio, and F. Cecchi, "Application of membrane bioreactor technology for wastewater treatment and reuse in the Mediterranean region: focusing on removal efficiency of non-conventional pollutants," *Journal of Environmental Management*, vol. 91, no. 12, pp. 2424–2431, 2010.

[13] A. Mudhoo, V. K. Garg, and S. Wang, *Heavy Metals: Toxicity and Removal by Biosorption*, In Environmental Chemistry for a Sustainable World (Pp. 379-442), Springer, Dordrecht, 2012.

[14] M. J. Ebrahimi Zarandi, M. R. Sohrabi, M. Khosravi, N. Mansouriieh, M. Davallo, and A. Khosravan, "Optimizing Cu (II) removal from aqueous solution by magnetic nanoparticles immobilized on activated carbon using Taguchi method," *Water Science and Technology*, vol. 74, no. 1, pp. 38–47, 2016.

[15] A. B. Bejaxhin, G. Paulraj, and M. Prabhakar, "Inspection of casting defects and grain boundary strengthening on stressed Al6061 specimen by NDT method and SEM micrographs," *Journal of Materials Research and Technology*, vol. 8, no. 3, pp. 2674–2684, 2019.

[16] P. Sureshkumar, T. Jagadeesha, L. Natrayan, M. Ravichandran, D. Veeman, and S. M. Muthu, "Electrochemical corrosion and tribological behaviour of AA6063/Si3N4/Cu (NO3) 2 composite processed using single-pass ECAPA route with 120° die angle," *Journal of Materials Research and Technology*, vol. 16, pp. 715–733, 2022.

[17] S. S. Baral, S. N. Das, and P. Rath, "Hexavalent chromium removal from aqueous solution by adsorption on treated sawdust," *Biochemical Engineering Journal*, vol. 31, no. 3, pp. 216–222, 2006.

[18] G. B. Adebayo, H. I. Adegoke, and S. Fauzeeyat, "Adsorption of Cr (VI) ions onto goethite, activated carbon and their composite: kinetic and thermodynamic studies," *Applied Water Science*, vol. 10, no. 9, pp. 1–18, 2020.

[19] N. Nasseh, R. Khosravi, G. A. Rumman et al., "Adsorption of Cr (VI) ions onto powdered activated carbon synthesized from Peganum harmala seeds by ultrasonic waves activation," *Environmental Technology & Innovation*, vol. 21, p. 101277, 2021.

[20] G. Bharath, K. Rambabu, F. Banat, A. Hai, A. F. Arangadi, and N. Ponpandian, "Enhanced electrochemical performances of peanut shell derived activated carbon and its Fe3O4 nanocomposites for capacitive deionization of Cr (VI) ions," *Science of the Total Environment*, vol. 691, pp. 713–726, 2019.

[21] Y. Wang, C. Peng, E. Padilla-Ortega, A. Robledo-Cabrera, and A. López-Valdivieso, "Cr (VI) adsorption on activated carbon: mechanisms, modeling and limitations in water treatment," *Journal of Environmental Chemical Engineering*, vol. 8, no. 4, p. 104031, 2020.

[22] A. Kumar and H. M. Jena, "Adsorption of Cr (VI) from aqueous phase by high surface area activated carbon prepared by chemical activation with ZnCl2," *Process Safety and Environmental Protection*, vol. 109, pp. 63–71, 2017.

[23] K. M. Doke and E. M. Khan, "Equilibrium, kinetic and diffusion mechanism of Cr (VI) adsorption onto activated carbon derived from wood apple shell," *Arabian Journal of Chemistry*, vol. 10, pp. S252–S260, 2017.

[24] M. Manjuladevi, R. Anitha, and S. Manonmani, "Kinetic study on adsorption of Cr (VI), Ni (II), Cd (II) and Pb (II) ions from aqueous solutions using activated carbon prepared from Cucumis melo peel," *Applied Water Science*, vol. 8, no. 1, pp. 1–8, 2018.

[25] M. Jain, M. Yadav, T. Kohout, M. Lahtinen, V. K. Garg, and M. Sillanpää, "Development of iron oxide/activated carbon nanoparticle composite for the removal of Cr (VI), Cu (II) and Cd (II) ions from aqueous solution," *Water Resources and Industry*, vol. 20, pp. 54–74, 2018.

[26] K. Simeonidis, E. Kaprara, T. Samaras et al., "Optimizing magnetic nanoparticles for drinking water technology: the case of Cr (VI)," *Science of the Total Environment*, vol. 535, pp. 61–68, 2015.

[27] X. Zhang, J. Wang, R. Li et al., "Preparation of Fe3O4@ C@ layered double hydroxide composite for magnetic separation of uranium," *Industrial & Engineering Chemistry Research*, vol. 52, no. 30, pp. 10152–10159, 2013.

[28] C. Guo, L. Ding, X. Jin, H. Zhang, and D. Zhang, "Application of response surface methodology to optimize chromium (VI) removal from aqueous solution by cassava sludge-based activated carbon," *Journal of Environmental Chemical Engineering*, vol. 9, no. 1, p. 104785, 2021.

[29] R. Suryanarayanan and V. G. Sridhar, "Effect of process parameters in pinless friction stir spot welding of Al 5754-Al 6061 alloys," *Metallography, Microstructure, and Analysis*, vol. 9, no. 2, pp. 261–272, 2020.

[30] I. Langmuir, "The adsorption of gases on plane surfaces of glass, mica and platinum," *Journal of the American Chemical Society*, vol. 40, no. 9, pp. 1361–1403, 1918.

[31] V. S. Nadh, C. Krishna, L. Natrayan et al., "Structural behavior of nanocoated oil palm shell as coarse aggregate in lightweight concrete," *Journal of Nanomaterials*, vol. 2021, 7 pages, 2021.

[32] S. A. Cavaco, S. Fernandes, M. M. Quina, and L. M. Ferreira, "Removal of chromium from electroplating industry effluents by ion exchange resins," *Journal of Hazardous Materials*, vol. 144, no. 3, pp. 634–638, 2007.

[33] A. I. Hafez, M. S. El-Manharawy, and M. A. Khedr, "RO membrane removal of unreacted chromium from spent tanning effluent. A pilot-scale study, part 2," *Desalination*, vol. 144, no. 1-3, pp. 237–242, 2002.

[34] P. Lakshmipathiraj, G. B. Raju, M. R. Basariya, S. Parvathy, and S. Prabhakar, "Removal of Cr (VI) by electrochemical reduction," *Separation and Purification Technology*, vol. 60, no. 1, pp. 96–102, 2008.

[35] Z. Song, C. J. Williams, and R. G. J. Edyvean, "Treatment of tannery wastewater by chemical coagulation," *Desalination*, vol. 164, no. 3, pp. 249–259, 2004.

[36] P. Venkateswaran and K. Palanivelu, "Solvent extraction of hexavalent chromium with tetrabutyl ammonium bromide from aqueous solution," *Separation and Purification Technology*, vol. 40, no. 3, pp. 279–284, 2004.

[37] A. B. Bejaxhin and G. Paulraj, "Effect of optimised cutting constraints by AlCrN/epoxy coated components on surface roughness in CNC milling," *International Journal of Rapid Manufacturing*, vol. 8, no. 4, pp. 397–417, 2019.